Physica A 391 (2012) 2720–2729

Contents lists available at SciVerse ScienceDirect

Physica A

journal homepage: www.elsevier.com/locate/physa

Cellular automata simulation of traffic including cars and bicycles

Jelena Vasic *, Heather J. Ruskin

School of Computing, Dublin City University, Glasnevin, Dublin 9, Ireland

ARTICLE INFO

Article history:
Received 10 January 2011
Received in revised form 3 December 2011
Available online 14 December 2011

Keywords:
Traffic flow
Urban traffic
Bicycle traffic
Discrete stochastic model
Simulation
Cellular automata

ABSTRACT

As 'greening' of all aspects of human activity becomes mainstream, transportation science is also increasingly focused around sustainability. Modal co-existence between motorised and non-motorised traffic on urban networks is, in this context, of particular interest for traffic flow modelling. The main modelling problems here are posed by the heterogeneity of vehicles, including size and dynamics, and by the complex interactions at intersections. Herein we address these with a novel technique, based on one-dimensional cellular automata components, for modelling network infrastructure and its occupancy by vehicles. We use this modelling approach, together with a corresponding vehicle behaviour model, to simulate combined car and bicycle traffic for two elemental scenarios—examples of components that would be used in the building of an arbitrary network. Results of simulations performed on these scenarios, (i) a stretch of road and (ii) an intersection causing conflict between cars and bicycles sharing a lane, are presented and analysed.

1. Introduction

Successful incorporation of alternative modes of transportation into urban traffic systems has become an important part of contemporary transport policy-making [1], owing to the beneficial effects of the use of alternatives to motorised vehicles. The benefits include those in the areas of health [2] and sustainability [3,4], but, while these are universal, the existing conditions relating to alternative modes, including infrastructure, attitudes and volumes, differ greatly from city to city [5–7] and also require different models of traffic flow, for example, to reflect the intermingled nature of the motorised–non-motorised traffic mix [8,9] or high-density bicycle flows [10].

Cellular automata (CA) models have been used widely for the representation of urban traffic since the publication of the seminal papers by Nagel and Schreckenberg [11] and Biham et al. [12], the former proposing a one-dimensional and the latter a two-dimensional model. Discrete in space and time, cellular automata models are suitable for computer simulation and have been applied since to successfully reproduce traffic phenomena [13], both qualitatively and quantitatively.

Highway traffic and traffic of urban networks have different characteristics, and are investigated separately, with the latter greatly affected by network topology and, both signal-aided and rule-based, control strategies. Urban systems and signal optimisation have been studied extensively, with CA [14–22] and by other types of models [23–25]. Nevertheless, the investigation of single intersections is an important part of understanding the dynamics of urban traffic [26] and how these build.

Interactions at unsignalised intersections and roundabouts have been studied using CA models for (i) homogeneous traffic [27–32] and (ii) heterogeneous cases [33–36].

Mixed motorised and non-motorised traffic also has been modelled using cellular automata: Gundaliya et al. [8] and Mallikarjuna and Rao [9] developed models, with multiple cell occupancy, reflecting size and shape of different vehicles, to reproduce the macroscopic properties of heterogeneous traffic typical of Indian cities. Further, bicycle flow characteristic of

* Corresponding author. Tel.: +353 17006747; fax: +353 17005442.
E-mail address: jelena.vasic@computing.dcu.ie (J. Vasic).

0378-4371/$ – see front matter
doi:10.1016/j.physa.2011.12.018

developing countries was modelled using Burgers CA [37] in Ref. [38], to reflect the 'in bulk' movements of bicycles. That same flow model for bicycles was combined in Ref. [36] with Velocity Dependent Randomisation (VDR) rules, proposed in Ref. [39], for cars, with a view to examining interactions between the two vehicle types at an intersection, where conflict exists between right-turning cars and straight-moving bicycles.

A similar problem to that studied in Ref. [36] was examined using a two-dimensional car-following model in Ref. [10]. This model allows for interactions between motorised and non-motorised vehicles in two dimensions and includes impact of other vehicles positioned laterally and behind, when determining the behaviour of any individual unit.

In this paper, we present a cellular automata-based model for combined car and bicycle traffic, under the specific conditions of sparse bicycle flows and road sharing by the two vehicle types based on 'positional discipline', which implies that bicycles keep to the side of the road nearest to the kerb, while cars allow space for any present bicycles by staying as far away from the kerb as possible.[1]

The ultimate aim of our research is to produce a scalable urban network simulation model for traffic including bicycles. We start with the already well tested [13] assumption that the basic movements of vehicles on a single-lane stretch of road can be approximated using a one dimensional cellular automata model and try to address the other modelling problems presented by the overall scenario, namely, the representation of:

(i) the difference in vehicle size and behaviour,
(ii) manoeuvres and interactions at intersections, and
(iii) lateral interactions between cars and bicycles sharing a lane.

The model presented here tackles these features of the problem domain by, respectively, (i) including cellular automata (CA) spaces with *differently sized cells*, (ii) representing intersections as a collection of geometrically natural CA spaces, and so allowing for the *extraction of the complexity of interactions from the geometry in a systematic way*, as opposed to the more usual superimposition of complex interactions on a relatively simple spatial representation of the intersection space and (iii) including the *relationship between two CA spaces* as a type of model element and allowing the definition of relationship type values, such as "unrelated", "sharing a wide road" or "sharing a narrow road", so that, for example, the presence of the latter value in the spatial model would invoke lateral interaction rules for bicycles and motorised traffic on relevant CA spaces. The spatial modelling approach is applicable to any type of intersection or other network feature. It also facilitates a general behaviour model, which does not need to be extended with the addition of new intersection types to the network: since the interactions are defined through the already mentioned extraction of information from the spatial representation, and that representation is based on a finite number of element types, the knowledge of these allows a vehicle to traverse arbitrary networks thus modelled.

We shall examine the properties of some basic examples built using this modelling approach. The two scenarios are (i) a road section with periodic boundary conditions, which is used to demonstrate the car–bicycle interaction model, and (ii) a left turn, which represents one of the simplest examples of an intersection at which bicycle–car interaction takes place.

Sections 2 and 3 of this paper describe, respectively, the spatial and vehicle behaviour models. The simulation scenarios and results are presented in Section 4. Section 5 concludes the paper, including an outline of the planned future context for the results presented here.

2. Spatial model

The spatial model is presented here at meta-level, that is, through the constructs that we use to model a road network space. A spatial model of an arbitrary network that serves heterogeneous traffic can be built using these six *spatial modelling constructs*. This is realised through transposition of sketches of the modelled infrastructure's natural geometry into a form comprising the spatial modelling constructs. What follows are the spatial modelling construct definitions, which include illustrations of the transposition method, based on pictures in Fig. 1.

1. The basic building-block of the spatial model is the one-dimensional cellular automata space, here called a *track*. Each route that a vehicle can take in the model is represented by a track, consisting of a sequence of cells of a certain size, numbered 1, 2 etc. This growing sequence of cell indices determines the direction of travel on the track. Each track is associated with one or more *vehicle types* of a size corresponding to the track's cell size. Cells in different tracks can be of different sizes, to accommodate different vehicle type sizes. The illustrations in Fig. 1 each contain one or more tracks.
2. *Turns* on a route have bearing on the dynamics of a vehicle's movement, hence are included as a spatial modelling construct. A descriptor for the turn with identifier i_T is defined as a pair of values:

$$D^T_{i_T} := (r^T_{i_T}, c^T_{i_T}) \tag{1}$$

where $r^T_{i_T}$ is the identifier of the track that the turn is on and $c^T_{i_T}$ is the index of the first cell of the turn. For example, the turn in Fig. 1(b) has the descriptor $(2, m + 3)$.

[1] In this paper, we refer to the sides of the road occupied by bicycles and cars as left and right, respectively, which corresponds to Irish driving, without loss of generality.

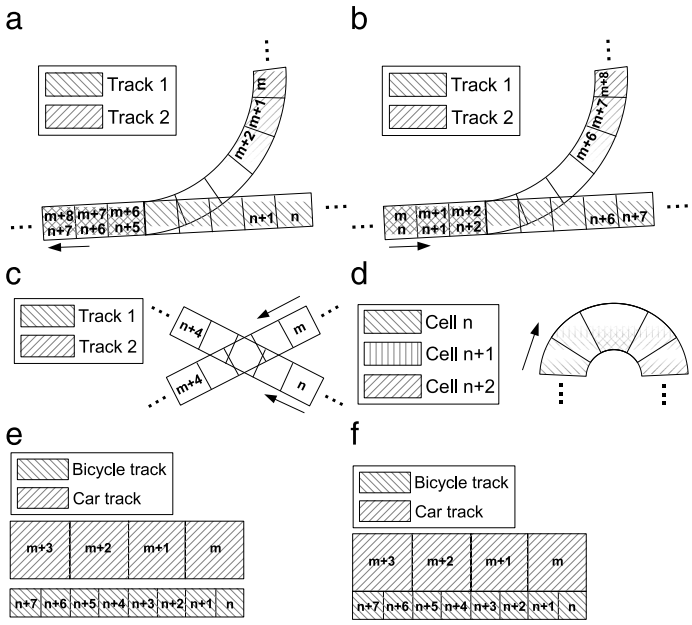

Fig. 1. Spatial modelling construct examples: (a) a merge of two one way streets, (b) a divergence of two one-way streets, (c) an intersection of two one way streets, (d) a sharp bend in a one-way street, (e) a portion of a wide one-way street shared between bicycles and cars with positional discipline and (f) a portion of a narrow one-way street shared in the same way. The arrows show track orientation. n and m are, in all cases, positive whole numbers, the value of which depends on where in the tracks the illustrated construct occurs.

3. Points in the network where vehicles might contend for simultaneous entrance into the same space are modelled using the *conflict* construct. We define the descriptor of the conflict with identifier i_{C} as a set of two pairs of values:

$$D^{\mathrm{C}}_{i_{\mathrm{C}}} := \{(r^{\mathrm{C}}_{i_{\mathrm{C}},1}, c^{\mathrm{C}}_{i_{\mathrm{C}},1}), (r^{\mathrm{C}}_{i_{\mathrm{C}},2}, c^{\mathrm{C}}_{i_{\mathrm{C}},2})\} \tag{2}$$

where $r^{\mathrm{C}}_{i_{\mathrm{C}},1}$ and $r^{\mathrm{C}}_{i_{\mathrm{C}},2}$ are identifiers of the two tracks involved in the conflict while $c^{\mathrm{C}}_{i_{\mathrm{C}},1}$ and $c^{\mathrm{C}}_{i_{\mathrm{C}},2}$ are the respective first cells (when viewing in direction of travel) in the conflict zone for tracks $r^{\mathrm{C}}_{i_{\mathrm{C}},1}$ and $r^{\mathrm{C}}_{i_{\mathrm{C}},2}$. The two value pairs in the conflict's descriptor each represent a distinct *view* of the conflict: $V^{\mathrm{C}}_{i_{\mathrm{C}},j} := (r^{\mathrm{C}}_{i_{\mathrm{C}},j}, c^{\mathrm{C}}_{i_{\mathrm{C}},j})$, where $j \in 1, 2$ is the identifier of the view. Conflicts arise if two tracks either merge or intersect. An example of the former is shown in Fig. 1(a) and of the latter in Fig. 1(c) and their descriptors are $(1, n+2)$, $(2, m+3)$ and $(1, n+1)$, $(2, m+1)$ respectively.
4. A *track relationship type* is defined for each specific way in which relative geometric positioning of two tracks can be the cause of some behaviour on the part of vehicles on either or both of those tracks. For example, Fig. 1(e) and (f) show spatial models for road sharing between bicycles and cars based on positional discipline. No track relationship types are involved in the former, even though the two tracks belong to the same road, as there is enough space for comfortable side-by-side movement of all vehicles. In the latter, however, a relationship of type "joined side-by-side" is assigned to the car and bicycle track pair and this will affect the dynamics of the vehicles on the two tracks.
5. As this is a model where tracks are based on the natural geometry of the modelled infrastructure, cells of different tracks can overlap. Each pair of overlapping cells are recorded in the model as an *instance of cell overlap*. For example, in Fig. 1(a), cell $n+5$ of Track 1 and cell $m+6$ of Track 2 overlap. The model also allows for overlap between cells on the same track. This is used to model "slowing" features of the road network, such as a turn. An acute bend modelled using three overlapping cells is shown in Fig. 1(d).
6. Some vehicle routes are identical up to a certain point, after which they diverge. Such points are specified in the model using the *divergence* construct. The descriptor of the divergence identified as i_{D} in the model, consisting of n diverging tracks, is defined as

$$D^{\mathrm{D}}_{i_{\mathrm{D}}} := \{(r^{\mathrm{D}}_{i_{\mathrm{D}},1}, c^{\mathrm{D}}_{i_{\mathrm{D}},1}, s^{\mathrm{D}}_{i_{\mathrm{D}},1}), (r^{\mathrm{D}}_{i_{\mathrm{D}},2}, c^{\mathrm{D}}_{i_{\mathrm{D}},2}, s^{\mathrm{D}}_{i_{\mathrm{D}},2}) \ldots (r^{\mathrm{D}}_{i_{\mathrm{D}},n}, c^{\mathrm{D}}_{i_{\mathrm{D}},n}, s^{\mathrm{D}}_{i_{\mathrm{D}},n})\} \tag{3}$$

where $r^{\mathrm{D}}_{i_{\mathrm{D}},j}$ identifies the jth diverging track, $c^{\mathrm{D}}_{i_{\mathrm{D}},j}$ is the index of the first cell (in the direction of travel) of the 'diverged' section of the jth diverging track and $s^{\mathrm{D}}_{i_{\mathrm{D}},j}$ is a semantic descriptor of the direction taken by the jth diverging track after the divergence, for example "straight" or "left". Fig. 1(b) shows an example of a divergence, which has the descriptor $(1, n+3$, "straight"$)$, $(2, m+3$, "left"$)$.

While the first five constructs listed above have an impact on the dynamics of traffic flow along individual routes in the modelled space, the last one allows the building of a view of the network structure, needed for the expression of navigation rules.

2.1. Traffic control considerations

Control features present in a road traffic network can be viewed as a layer superimposed onto the spatial aspect of the infrastructure, introducing constraints on how the space can be used by vehicles. Control devices of priority and traffic lights can be included in the conflict model.

- In the case of priority given to one of the tracks in a conflict, from the point of view of that track the conflict is always resolved.
- In the case of a traffic light, the conflict is resolved for the track under the green phase and unresolved for the track under the red one.

3. Vehicle behaviour model

As a vehicle navigates a network defined using the spatial model, it moves along a route that is, in fact, a one-dimensional cellular automata (CA) space (transversal movements, which are not currently considered as part of the model, would involve 'track hopping'). The movement rules are based on the original Nagel–Schreckenberg [11] rules. Even though these do not reproduce all the properties of traffic flow on freeways, they are sufficient as a base for the purpose of modelling movement in an urban network [13]. They can be summarised as follows.

1. Acceleration: if $v_i < v_{\mathrm{MAX}}$ and $v_i < d_i$, $v_i \to v_i + 1$.
2. Slowing (due to cars ahead): if $d_i < v_i$, $v_i \to d_i$.
3. Randomisation: if $v_i > 0$, with probability p_{R}, $v_i \to v_i - 1$.
4. Vehicle motion: each vehicle is advanced v_i cells along the track

where v_i is the velocity of the ith vehicle, v_{MAX} is the maximal velocity, d_i is the number of free cells between the ith vehicle and the vehicle ahead of it on the track and p_{R} is the randomisation parameter, used to introduce stochasticity into the model. All the variables are dimensionless, the velocities representing the number of cells traversed per time unit. At each time step of the simulation the rules are applied to each vehicle in the system.

We use these rules as a basis for a model of heterogeneous traffic on a network. The subsections below describe different aspects of the model and its application.

3.1. General considerations

The first three rules of the Nagel–Schreckenberg model have the purpose of velocity update, while the last rule updates the vehicle position, i.e. the cell that it occupies. Position update can be performed (i) in parallel for each time step, where first the velocities for all the vehicles in the system are determined, then all the vehicles are moved or (ii) in sequence, where each vehicle moves immediately upon determining its velocity for the time step. We chose the more commonly used parallel update, because it is "less safe" from the point of view of conflict resolution, and thus more closely models the problems of interest here.

The same rules are applied to bicycles and cars. The difference between the two types of vehicle is modelled in the different values for v_{MAX}, 3 for cars and 2 for bicycles, and in differently sized cells: car cells are made to represent 7.5 m long lengths of road, while bicycle cells are half the length of car cells, corresponding to 3.75 m on a real road. The time step corresponds to a real time interval of 1 s, which makes the maximal velocities for cars and bicycles 81 km/h and 27 km/h, respectively.

3.2. Movement on a track

The first two Nagel–Schreckenberg rules can be viewed as if based on a combined limiting value, contributed to by the maximal velocity and the distance to the vehicle ahead, and can be re-formulated as follows, into a *single-limit form of the N–S rules*:

1. Acceleration: if $v_i < v_{\mathrm{L}i}$, $v_i \to v_i + 1$.
2. Slowing: if $v_i > v_{\mathrm{L}i}$, $v_i \to v_{\mathrm{L}i}$.
3. Randomisation: if $v_i > 0$, with probability p_{R}, $v_i \to v_i - 1$.
4. Vehicle motion: each vehicle is advanced v_i cells along the track

where, $v_{\mathrm{L}i} = \min(v_{\mathrm{MAX}}, d_i)$.

We modify the Nagel–Schreckenberg rules through re-defining the way this limiting velocity value for the ith vehicle, $v_{\mathrm{L}i}$, is calculated:

$$v_{\mathrm{L}i} = \min(v_{\mathrm{MAX}}, d_{\mathrm{U}i}, v_{\mathrm{L}}^{\mathrm{T}}(d_i^{\mathrm{T}}), v_{\mathrm{L}}^{\mathrm{C}}(d_i^{\mathrm{C}})) \tag{4}$$

where d_i^{T} is the distance to the nearest turn ahead of the vehicle, $v_{\mathrm{L}}^{\mathrm{T}}(d_i^{\mathrm{T}})$ is a function of that distance and represents the velocity limit imposed by the turn, d_i^{C} is the distance to the nearest *unresolved* conflict ahead of the vehicle, $v_{\mathrm{L}}^{\mathrm{C}}(d_i^{\mathrm{C}})$ is a function of that distance and represents the velocity limit imposed by the conflict and, finally, $d_{\mathrm{U}i}$ is the number of *unimpinged* cells ahead of the vehicle. A cell is unimpinged if it is not occupied and if no other cells overlapping it

Table 1
Velocity limits for vehicles as a function of distance to the limit-imposing item. These velocity limits are denoted as $v_L^T(d_i^T)$, $v_L^C(d_i^C)$ and $v_L^B(d_i^B)$, corresponding to turns, conflicts and bicycles, respectively, as limiting factors. The numbers in the heading row represent the distance. The velocity limits were chosen so as to allow a vehicle to reach the velocity of 1 at the cell before a turn or bicycle and the velocity of 0 at the cell before an unresolved conflict, by decelerating, at most, by 1. The table applies to the case of $v_{MAX} = 3$ for cars and $v_{MAX} = 2$ for bicycles. For distance values not shown in the table, as for the particular cases indicated by the symbol ∞, no limiting value applies.

d_i^T or d_i^C or d_i^B	6	5	4	3	2	1	0
$v_L^T(d_i^T)$, where ith vehicle is a car	∞	2	2	2	1	1	∞
$v_L^C(d_i^C)$, where ith vehicle is a car	2	2	2	1	1	0	∞
$v_L^T(d_i^T)$, where ith vehicle is a bicycle	∞	∞	∞	∞	1	1	∞
$v_L^C(d_i^C)$, where ith vehicle is a bicycle	∞	∞	∞	1	1	0	∞
$v_L^B(d_i^B)$, where ith vehicle is a car	∞	2	2	2	1	1	1

are occupied. The functions $v_L^T(d_i^T)$ and $v_L^C(d_i^C)$ used in our simulations are shown in tabular form in rows 1–4 of Table 1. The distance arguments, d_i^T and d_i^C, impingement and conflict resolution will now be discussed in some detail.

The checking of impingement relies on information about instances of cell overlap. In the implementation, this can be performed efficiently by grouping overlap instances into bit-fields corresponding to areas where a lot of overlap occurs, such as intersections.

With use of the spatial modelling construct descriptor notation introduced in Section 2, the distance arguments are defined as follows. The ith vehicle's *distance from the nearest turn* is $d_i^T = c^T_{i_{T1}(i)} - c_i$, where c_i is the cell position of the ith vehicle and $i_{T1}(i)$ is the identifier of the nearest turn ahead of the vehicle. The *turn* spatial modelling construct descriptor component $c^T_{i_{T1}(i)}$ is the index of that turn's first cell. In the turn example in Fig. 1(b), if vehicle i is in cell m and the turn in Track 1 is given the identifier 1, $d_i^T = c_1^T - c_i = (m+3) - m = 3$. The ith vehicle's distance *from the nearest unresolved conflict* is $d_i^C = c^C_{i_{C1}(i),t_{C1}(i)} - c_i$, where c_i is the cell position of the ith vehicle, $i_{C1}(i)$ is the identifier of the nearest unresolved conflict ahead of the vehicle and $t_{C1}(i)$ is the conflict-specific identifier of the track on which the ith vehicle is moving. The *conflict* spatial modelling construct descriptor component $c^C_{i_{C1}(i),t_{C1}(i)}$ is the index of the first conflict-zone cell for that track. In the example based on Fig. 1(a), given in the previous paragraph, if the ith vehicle is in cell $n+1$ of Track 1 and the conflict is given the identifier 1, the vehicle's distance to the conflict is $d_i^C = c^C_{1,1} - c_i = (n+2) - (n+1) = 1$.

Whether a conflict is resolved or not is clear in cases where signalisation is present and for tracks with priority, as explained in Section 2.1. Where signalisation is absent, a vehicle approaching on a lower-priority track must employ some criterion to determine the state of a conflict. Our model uses the following rule: the conflict is considered *unresolved* if a vehicle on the conflicting track may enter the conflict zone in the next time step. For example, a vehicle approaching the conflict in Fig. 1(a) on Track 1, occupying cell $n+1$, would see the conflict as unresolved if a vehicle is in cell $m+1$ of Track 2, moving with a velocity greater than 0 (even if its velocity is currently 1, this may increase to 2 during the current update, in which case the vehicle would move to cell $m+3$, entering the conflict zone). We call this conflict resolution approach *soft yield*, as it is effectively the avoidance of crashes without courteousness on the part of the yielding flow, in that the higher-priority flow may be somewhat impeded. This is, in our estimation, a fair model of cyclist–driver interactions at conflict points. The more usual gap acceptance approach is to include full clearing of the conflict area as a requirement [40].

3.3. Network navigation

If there is a divergence ahead of a moving vehicle and the vehicle's journey does not end at a point between its current position and the position of the divergence, the vehicle must decide which of the diverging tracks it will take. In the model, the decision is made at the earliest time-step in which the vehicle is on the stretch of track preceding the divergence and is based on probabilities assigned to the different diverging tracks.

3.4. Car–bicycle interaction

The final factor that must be taken into account in the model is car–bicycle interaction. Bicycles and cars are considered not to be affected by each other, except in the case of narrow street sharing between the two modes, corresponding to track relationship type of "joined side-by-side" introduced in Section 2, where cars decelerate in the presence of bicycles. We use two different models to represent this effect.

1. In this version of the model, a bicycle imposes a velocity limit on a car based on the longitudinal distance between them, in the same way as a turn or conflict would. Eq. (4), *for cars only*, becomes:

$$v_{Li} = \min(v_{MAX}, d_{Ui}, v_L^T(d_i^T), v_L^C(d_i^C), v_L^B(d_i^B)) \tag{5}$$

where d_i^{B} is the longitudinal distance from car to bicycle and $v_{\mathrm{L}}^{\mathrm{B}}(d_i^{\mathrm{B}})$ the bicycle-imposed velocity limit for a car. The values of $v_{\mathrm{L}}^{\mathrm{B}}(d_i^{\mathrm{B}})$ are given in row 5 of Table 1, while $d_i^{\mathrm{B}} = c_{i_{\mathrm{B1}}(i)}^{\mathrm{C}} - c_i$, where c_i is the index of the cell occupied by the car and $c_{i_{\mathrm{B1}}(i)}^{\mathrm{C}}$ is the index of the cell in the car track that is positioned alongside the longitudinally nearest bicycle ahead of the car, the superscript C denoting that the cell index is in the car track and $i_{\mathrm{B1}}(i)$ denoting the vehicle index of the longitudinally nearest bicycle ahead of the ith car. If, in the example in Fig. 1(f), a car is in cell m of the car track, cells n to $n+4$ of the bicycle track are empty and there is a bicycle in cell $n+5$ of the bicycle track, then $d_i^{\mathrm{B}} = (m+2) - m = 2$. With a car in the same position as in the previous example and a bicycle in cell n, the distance would be $d_i^{\mathrm{B}} = m - m = 0$. This model of car–bicycle interaction is called the *limit-based model*.

2. This version of the model incorporates the effect of bicycles on cars into the randomisation rule. The velocity is calculated as it would be in the absence of bicycles in the first two rules. Then, if a bicycle is within a certain time headway, t_{H}, of the car,[2] the car's randomisation parameter, p_{R}, is increased to a specified value. This *adjusted randomisation parameter* value and the time headway are configurable parameters of the model. This model of car–bicycle interaction is called the *randomisation based model*.

4. Simulation results for two scenarios road stretch and left turn

Two scenarios are simulated: a road stretch with periodic boundary conditions and a left turn. Each is defined in terms of the spatial modelling constructs from Section 2, together with relevant performed simulations and results, in a separate subsection.

Simulation length in all cases was 10^4 time-steps. The randomisation parameter base value used in all the simulations is $p_R = 0.1$. The measurements of the number of vehicles passing per time step, i.e. flow, were taken separately for cars and bicycles, at a single cell, and averaged over all the timesteps.

4.1. Road stretch with closed boundary conditions

The road stretch scenario is built around a spatial model like the one shown in Fig. 1(f), with periodic boundary conditions. This can be expressed in terms of spatial model constructs as follows:

1. *Tracks:* a 100 cell long car track and a 200 cell long bicycle track.
2. *Turns:* none. The ring formed by the closed road is large enough for the curve to be negligible.
3. *Conflicts:* none.
4. *Track relationships:* relationship of type "joined side-by-side" between car track and bicycle track, indicating that the road shared by bicycle and car with positional discipline is narrow.
5. *Instances of cell overlap:* in the car track, for $n > 0$, cell n overlaps with cell $n + 100$ and, similarly, in the bicycle track, for $m > 0$, cell m overlaps with cell $m + 200$.
6. *Divergences:* none.

Fig. 2 presents car-only fundamental diagrams,[3] as a function of bicycle density, for different car–bicycle interaction models. In all these models the presence of bicycles reduces average car flow but the mechanisms by which this is effected are different. In Fig. 2(a), the car fundamental diagram takes on the even-sided triangle shape of low-velocity traffic, brought about by the orderly slowing down of cars in the presence of bicycles, prescribed by the limit-based model. The diagrams in Fig. 2(b), (c) and (d) are all for the randomisation-based model of car–bicycle interaction and with higher bicycle densities tend towards congestion at low density values, caused by the stochastic nature of the car–bicycle interaction. We find that the time headway value does not affect the results almost at all (there is little or no difference between diagrams (b) and (c)), while the adjusted randomisation parameter is an important parameter of the model (compare diagrams (b) and (d)). Some combination of the two approaches may be needed for realistic calibration of the car–bicycle interaction model.

4.2. Left turn

The spatial model of the left turn scenario is shown in Fig. 3 and consists of a one-way narrow street shared between cars and bicycles, with a similar street perpendicularly branching out to the left, forming a left turn. This scenario can be defined using the spatial modelling constructs as follows.

1. *Tracks:* BS, BL, CS, CL, as shown in Fig. 3.
2. *Turns:* (BL, 201), (CL, 101).
3. *Conflicts:* (BS, 201), (CL, 101).
4. *Track relationships:* BS and CS: "joined side-by-side". BL and CL "joined side-by-side".

[2] This means that the car, at its currently calculated velocity, would be alongside the point where the bicycle currently is, within t_{H} time-steps.

[3] A fundamental diagram shows the flow, i.e. the average number of vehicles that pass a certain point in the road per time-step, as a function of vehicle density, which is the average number of vehicles that occupy a unit of length, measured at the same point in the road.

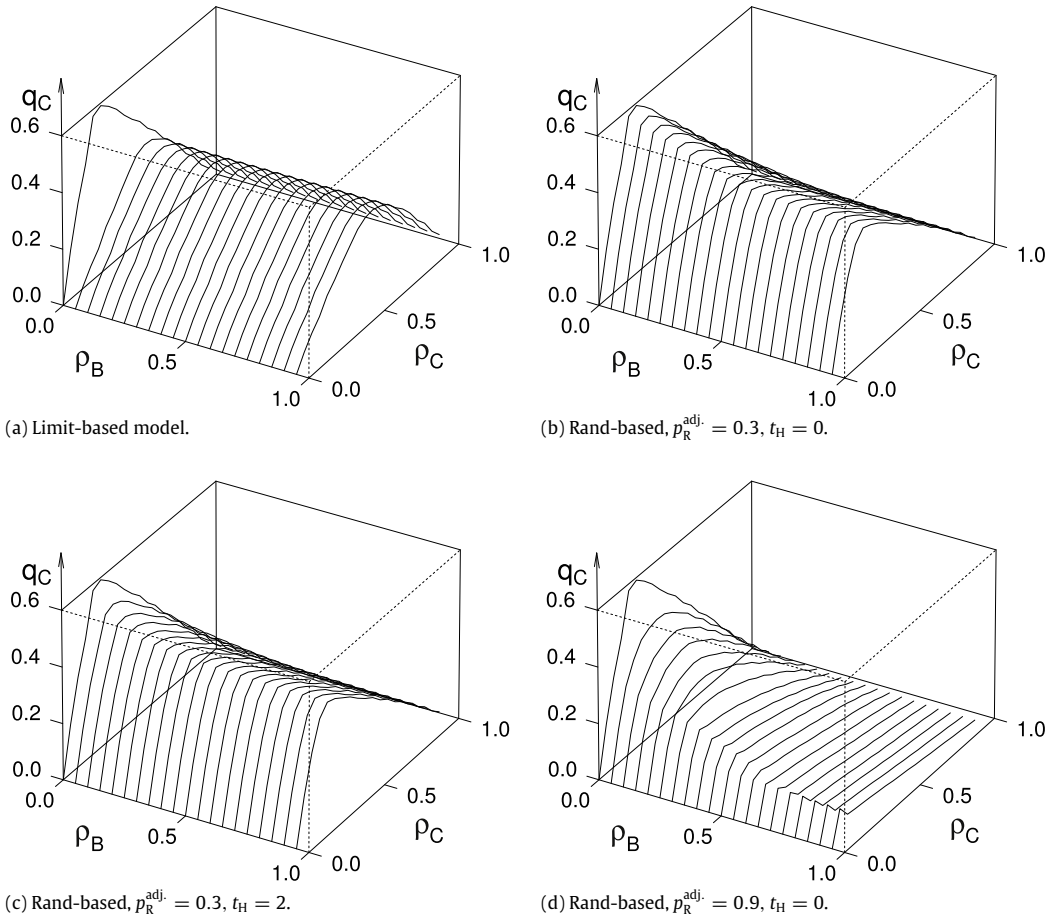

(a) Limit-based model.

(b) Rand-based, $p_R^{adj.} = 0.3$, $t_H = 0$.

(c) Rand-based, $p_R^{adj.} = 0.3$, $t_H = 2$.

(d) Rand-based, $p_R^{adj.} = 0.9$, $t_H = 0$.

Fig. 2. Road stretch with periodic boundary conditions: fundamental diagrams for cars as a function of bicycle density. With limit-based model of bicycle effect on cars (a) and with randomisation-based model of bicycle effect, using different values for adjusted randomisation parameter and time headway ((b), (c) and (d)). $p_R^{adj.}$ denotes the adjusted randomisation parameter in the randomisation-based interaction model, while t_H is the time headway.

Table 2
Cell overlap table for left turn shown in Fig. 3. Column and row headings refer to cells. A value of 1 indicates overlap between the cells referred to by the relevant column and row, while 0 indicates no overlap. The pairs of cells not shown in the table do not overlap.

	BS201	BS202	CS101	BL201	BL202	BL203	CL101	CL102	CL103
BS201	1	0	0	1	1	0	1	1	1
BS202	0	1	0	0	0	0	1	1	1
CS101	0	0	1	0	0	0	1	1	1
BL201	1	0	0	1	1	1	0	0	0
BL202	1	0	0	1	1	1	0	0	0
BL203	0	0	0	1	1	1	0	0	0
CL101	1	1	1	0	0	0	1	1	1
CL102	1	1	1	0	0	0	1	1	1
CL103	1	1	1	0	0	0	1	1	1

5. *Instances of cell overlap:* Overlap of cells is specified in Table 2.
6. *Divergences:* (BS, 201), (BL, 201), (CS, 101), (CL, 101).

One control feature is present in the scenario: track BS has priority over track CL at the conflict.

The measurements for the left turn scenario were taken at cells BS200 and CS100. The probability of turning for bicycles is set to 0.0. A new car(bicycle) is inserted with probability p_{IC} (p_{IB}) at every time-step. A new car is inserted, with velocity 2, either onto cell CS2 (if both CS2 and CS1 are empty), onto CS1 (if CS1 is empty and CS2 is occupied) or is discarded. A new bicycle is either placed onto cell BS1 (if that cell is empty) or discarded. Vehicles leave as if the tracks extend indefinitely and are always empty beyond cells CS201, BS402, CL203 and BS403.

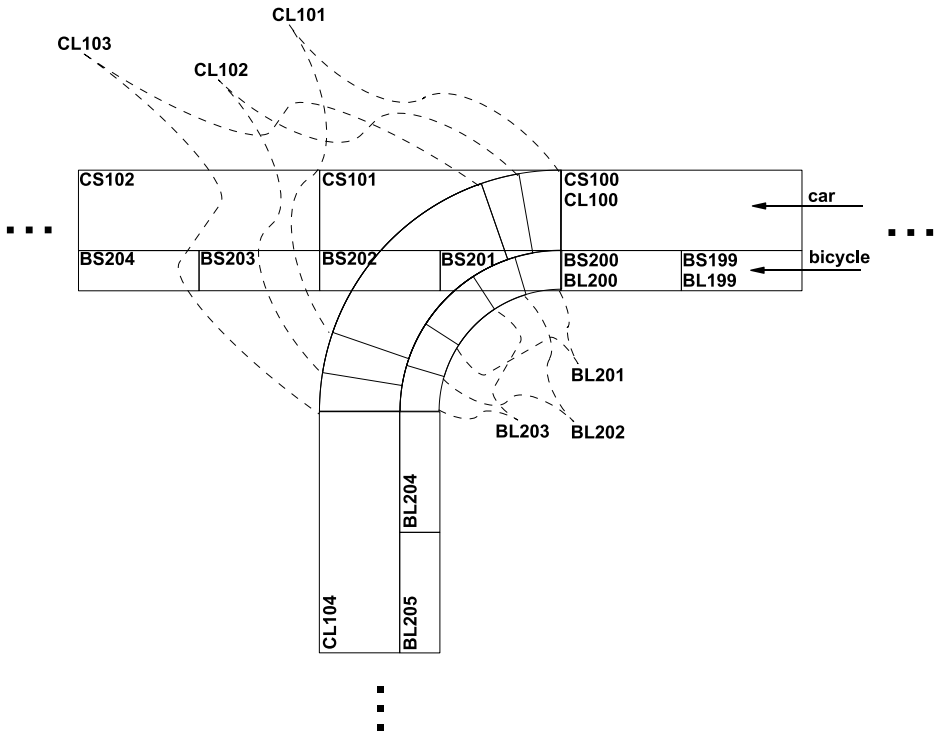

Fig. 3. Spatial model of the left turn scenario with road sharing and positional discipline on a narrow street (the bicycle and car tracks are deemed to have a relationship type of "joined side-by-side"). Cells are labelled using the format <track label><cell index>, where <track label> is one of BS, BL, CS and CL, which stand for track names "bicycle straight", "bicycle left", "car straight" and "car left", respectively, while <cell index> is a non-zero index of the cell within the track. The lengths of the tracks are BS-402, BL-403, CS-201 and CL-203. Tracks BL and CL contain overlapping cells.

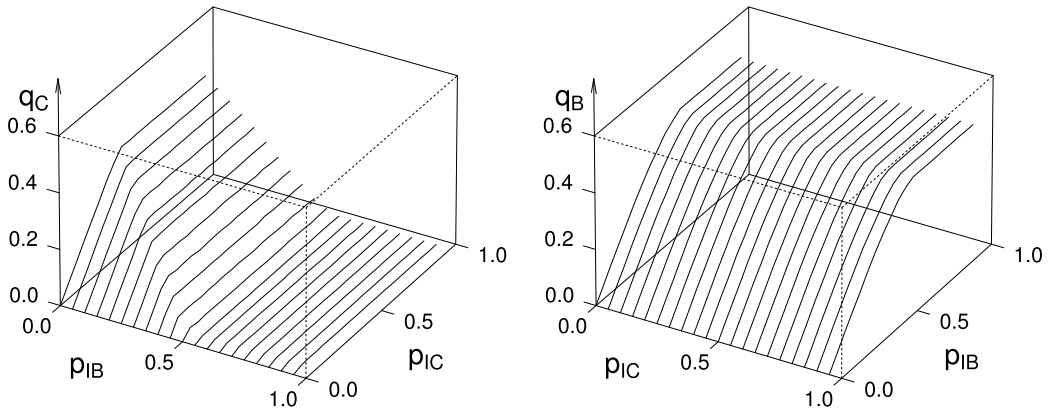

(a) Cars. (b) Bicycles.

Fig. 4. Left turn: flows for cars (a) and for bicycles (b), as a function of the other vehicle type's insertion probability, p_{IB} or p_{IC}. The diagrams are shown for the randomisation-based interaction model, with the adjusted randomisation parameter value $p_{\mathrm{R}} = 0.5$ and turning probability for car of $p_{\mathrm{T}} = 0.5$.

Fig. 4 shows how insertion probability/flow curves for cars and bicycles change in the function of the other vehicle type's insertion probability, for the left turn scenario. Because bicycles are given priority at this turn, the flow for cars is greatly reduced with an increase in bicycle insertion probability. Bicycle flows are largely unchanged by car insertion probabilities.

The diagrams formed from points in plane $p_{\mathrm{IC}} = 1.0$ in Fig. 4(a) represent car flow capacity diagrams. Fig. 5 shows how these diagrams change with car turning probability, p_{T}, and the turn cell count for cars, c_{T}. The turn cell count is the number of cells representing the curved part of the turn and is a measure of the difficulty of turning. While Fig. 3 shows the case where the car turning curve consists of three cells, CL101, CL102 and CL103, simulations have been performed for two other cases: a 2-cell car turn and a 1-cell car turn and car flow capacities are affected by this parameter. Also, the car flow capacity increases slightly with p_{IB} near $p_{\mathrm{IB}} = 1.0$. This is due to the almost uniform car velocities, limited to 1 in the presence of bicycles.

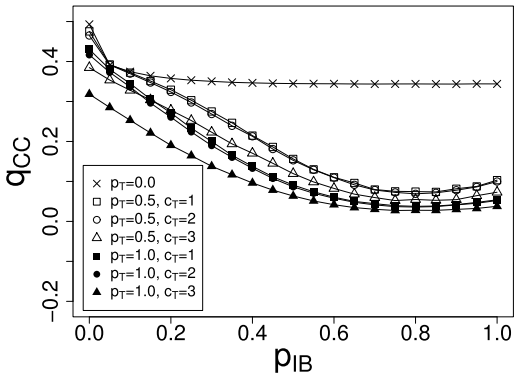

Fig. 5. Left turn: car flow capacity, as a function of the bicycle insertion rate, for different car turning probabilities, p_T and different turn cell counts, c_T, in the case of limit-based bicycle–car interaction.

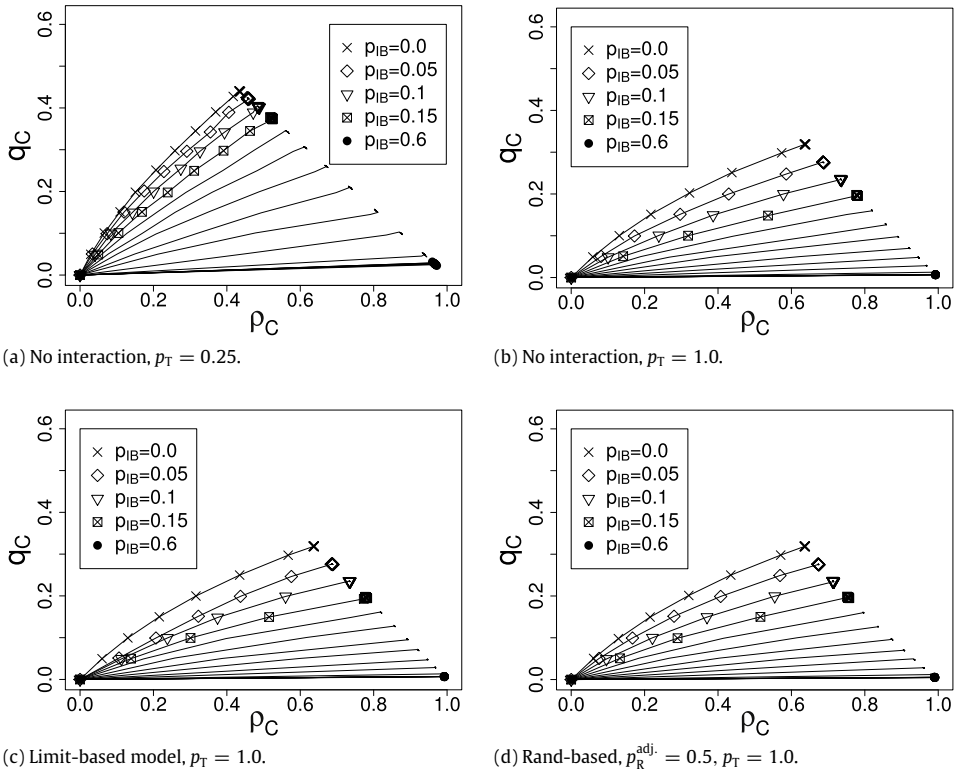

(a) No interaction, $p_T = 0.25$.

(b) No interaction, $p_T = 1.0$.

(c) Limit-based model, $p_T = 1.0$.

(d) Rand-based, $p_R^{adj.} = 0.5$, $p_T = 1.0$.

Fig. 6. Left turn: fundamental diagrams for cars. Car fundamental diagrams are shown for bicycle insert probability values of $0.0 \leq p_{IB} < 1.0$, with step 0.05. $p_R^{adj.}$ denotes the adjusted randomisation parameter in the randomisation-based interaction model, while t_H is the time headway. p_T is the turning probability for cars.

More information about what is actually happening at the entrance to the intersection can be gained from Fig. 6, which shows fundamental diagrams, that is, vehicle flow as a function of density at the point of measurement. The fact that the fundamental diagram lines for cars extend far into the high-density regions (Fig. 6(a), (b), (c) and (d)) indicate queuing by cars. Longer queues are accompanied by lower capacities, defined by the bicycle insertion probability and cars' probability of turning. The points shown for selected values of p_{IB} demonstrate that before reaching capacity, the flow of cars is unchanged by p_{IB}. Comparison of the four diagrams for cars shows that the car–bicycle interaction model type does not make a difference as to the flow values (Fig. 6(b), (c) and (d)), while the probability of turning for cars, expectedly, does (Fig. 6(a) as opposed to (b), (c) and (d)). In a network with many intersections, the dynamics observed in the road stretch simulations may become entirely irrelevant.

5. Conclusion

In this paper, we have presented a new approach to modelling heterogeneous traffic using cellular automata. With view to constructing models of large networks as the next step, we have devised a model that allows for extensibility and scalability, both of model and of implementation. While other research has investigated mixed traffic containing bicycles, it has not been done, to our knowledge, for the case of a city where bicycle facilities are scarce and sharing of roads is the most common form of bicycle inclusion, as is the case with many old European city centres, such as Dublin's. Neither has it been undertaken elsewhere with the aim of studying whole-network dynamics, which is needed if bicycles are to be encouraged and better facilitated within planning processes, today heavily oriented towards city 'greening'. The initial results we obtained for two basic scenarios show the general viability of the model. While the car–bicycle interaction model would, in general, require calibration with real data in the case of highway traffic, it may be the case that because intersection dynamics dominate the picture even at this simple level, the former could be discarded entirely in network simulations and calibration of city-wide models.

Acknowledgement

This work is funded by the Irish Research Council for Science, engineering and Technology (IRCSET), through an 'Embark Initiative' postgraduate scholarship.

References

[1] Ireland's first national cycle policy framework 2009–2020, Technical Report, Department of Transport, 2009.
[2] J. Pucher, J. Dill, S. Handy, Infrastructure, programs, and policies to increase bicycling: an international review, Prev. Med. 50 (2010) 106–125.
[3] L. Wright, L. Fulton, Climate change mitigation and transport in developing nations, Transport Rev. 25 (2005) 691–717.
[4] R. Massink, Estimating the climate value of bicycling in Bogota, Colombia, using a shadow pricing methodology, Master's Thesis, University of Twente, 2009.
[5] J. Zacharias, Bicycle in shanghai: movement patterns, cyclist attitudes and the impact of traffic separation, Transport Rev. 22 (2002) 309–322.
[6] J. Pucher, R. Buehler, Cycling for everyone: lessons from Europe, Transp. Res. Rec. 2074 (2008) 58–65.
[7] R. Cervero, O. Sarmiento, E. Jacoby, L. Fernando Gomez, A. Neiman, Influences of built environments on walking and cycling: lessons from Bogota, Int. J. Sustainable Transp. 3 (2009) 203–226.
[8] P. Gundaliya, T. Mathew, S. Dhingra, Heterogeneous traffic flow modelling for an arterial using grid based approach, J. Adv. Transp. 42 (2008) 467–491.
[9] C. Mallikarjuna, K. Rao, Cellular automata model for heterogeneous traffic, J. Adv. Transp. 43 (2009) 321–345.
[10] D. Xie, Z. Gao, X. Zhao, K. Li, Characteristics of mixed traffic flow with non-motorized vehicles and motorized vehicles at an unsignalized intersection, Physica A 388 (2009) 2041–2050.
[11] K. Nagel, M. Schreckenberg, A cellular automaton model for freeway traffic, J. Phys. I 2 (1992) 2221–2229.
[12] O. Biham, A. Middleton, D. Levine, Self-organization and a dynamical transition in traffic-flow models, Phys. Rev. A 46 (1992) R6124–R6127.
[13] S. Maerivoet, B. De Moor, Cellular automata models of road traffic, Phys. Rep. 419 (2005) 1–64.
[14] B. Chopard, P.O. Luthi, P.A. Queloz, Cellular automata model of car traffic in a two-dimensional street network, J. Phys. A 29 (1996) 2325–2336.
[15] J. Esser, M. Schreckenberg, Microscopic simulation of urban traffic based on cellular automata, Internat. J. Modern Phys. C 8 (1997) 1025–1036.
[16] P.M. Simon, K. Nagel, Simplified cellular automaton model for city traffic, Phys. Rev. E 58 (1998) 1286–1295.
[17] D. Chowdhury, A. Schadschneider, Self-organization of traffic jams in cities: effects of stochastic dynamics and signal periods, Phys. Rev. E 59 (1999) R1311–R1314.
[18] E. Brockfeld, R. Barlovic, A. Schadschneider, M. Schreckenberg, Optimizing traffic lights in a cellular automaton model for city traffic, Phys. Rev. E 64 (2001) 056132.
[19] J. Wahle, M. Schreckenberg, A multi-agent system for on-line simulations based on real-world traffic data, in: Hawaii International Conference on System Sciences, vol. 3, 2001, p. 3037.
[20] D.W. Huang, W.N. Huang, Traffic signal synchronization, Phys. Rev. E 67 (2003) 056124.
[21] O.K. Tonguz, W. Viriyasitavat, F. Bai, Modeling urban traffic: a cellular automata approach, IEEE Commun. Mag. 47 (2009) 142–150.
[22] S. Scellato, L. Fortuna, M. Frasca, J. Gómez-Gardeñes, V. Latora, Traffic optimization in transport networks based on local routing, Eur. Phys. J. B 73 (2010) 303–308.
[23] B. Toledo, V. Munoz, J. Rogan, C. Tenreiro, J. Valdivia, Modeling traffic through a sequence of traffic lights, Phys. Rev. E 70 (2004) 016107.
[24] T. Nagatani, Control of vehicular traffic through a sequence of traffic lights positioned with disordered interval, Physica A 368 (2006) 560–566.
[25] S. Laemmer, D. Helbing, Self-control of traffic lights and vehicle flows in urban road networks, J. Stat. Mech. 2008 (2008) P04019.
[26] M. Foulaadvand, M. Fukui, S. Belbasi, Phase structure of a single urban intersection: a simulation study, J. Stat. Mech. 2010 (2010) P07012.
[27] H. Ruskin, R. Wang, Modelling traffic flow at an urban unsignalised intersection, Lecture Notes in Comput. Sci. 2329 (2002) 381–390.
[28] R. Wang, H. Ruskin, Modeling traffic flow at a single-lane urban roundabout, Comput. Phys. Commun. 147 (2002) 570–576.
[29] R. Wang, H. Ruskin, Modelling traffic flow at a multilane intersection, Lecture Notes in Comput. Sci. 2667 (2003) 577–586.
[30] X. Li, R. Jiang, Q. Wu, Cellular automaton model simulating traffic flow at an uncontrolled t-shaped intersection, Internat. J. Modern Phys. B 18 (2004) 2703–2707.
[31] R. Wang, H. Ruskin, Modelling traffic flow at multi-lane urban roundabouts, Internat. J. Modern Phys. C 17 (2006) 693–710.
[32] X. Li, Z. Gao, B. Jia, X. Zhao, Cellular automata model for unsignalized t-shaped intersection, Internat. J. Modern Phys. C 20 (2009) 501–512.
[33] P. Deo, H. Ruskin, Simulation of heterogeneous motorised traffic at a signalised intersection, Lecture Notes in Comput. Sci. 4173 (2006) 522–531.
[34] P. Deo, H. Ruskin, Comparison of homogeneous and heterogeneous motorised traffic at signalised and two-way stop control single lane intersection, Lecture Notes in Comput. Sci. 3980 (2006) 622–632.
[35] Y. Feng, Y. Liu, P. Deo, H. Ruskin, Heterogeneous traffic flow model for a two-lane roundabout and controlled intersection, Internat. J. Modern Phys. C 18 (2007) 107–117.
[36] X. Li, Z. Gao, B. Jia, X. Zhao, Modeling the interaction between motorized vehicle and bicycle by using cellular automata model, Internat. J. Modern Phys. C 20 (2009) 209–222.
[37] K. Nishinari, D. Takahashi, Analytical properties of ultradiscrete burgers equation and rule-184 cellular automaton, J. Phys. A 31 (1998) 5439.
[38] R. Jiang, B. Jia, Q. Wu, Stochastic multi-value cellular automata models for bicycle flow, J. Phys. A 37 (2004) 2063.
[39] R. Barlovic, L. Santen, A. Schadschneider, M. Schreckenberg, Meta-stable states in cellular automata for traffic flow, Eur. Phys. J. B 5 (1998) 793–800.
[40] W. Brilon, R. Koenig, R. Troutbeck, Useful estimation procedures for critical gaps, Transp. Res. A 33 (1999) 161–186.